

# Boron-doped diamond electrodes for carbofuran electrochemical degradation

## Eletrodos de diamante dopado com boro para degradação eletroquímica do carbofurano

Nazir Monteiro dos Santos<sup>1\*</sup>, Marcos Roberto de Vasconcelos Lanza<sup>2</sup>, Neidênei Gomes Ferreira<sup>3</sup>, Maurício Ribeiro Baldan<sup>3</sup>

### ABSTRACT

Boron-doped diamond electrodes (BDD) were produced on titanium (Ti) substrate by Hot Filament Chemical Vapor Deposition (HFCVD) reactor for electrochemical degradation of carbofuran pesticide. The morphological and structural characterizations of the electrodes were evaluated by Scanning Electron Microscopy (SEM) and by Raman scattering Spectroscopy techniques. The apparent space charge density ( $N_A$ ) value was determined by Mott-Schottky Plot, in which was approximately  $10^{19} \text{ cm}^{-3}$ . The electrochemical characterization of electrodes was performed by Cyclic Voltammetry, and it was observed large potential windows. The electrochemical oxidation (EO) of the carbofuran were performed at different current densities, flow rates of 50 and  $300 \text{ Lh}^{-1}$  for a total of 2 hours with an electrolyte 0.1 M potassium sulfate ( $\text{K}_2\text{SO}_4$ ) aqueous solutions and  $1,8 \times 10^{-3} \text{ M}$  carbofuran in a flow reactor with recirculation. The efficiency of the pesticide degradation process was monitored by Ultraviolet-Visible Spectrophotometry (UV-Vis), Total Organic Carbon (TOC) and High Performance Liquid Chromatography (HPLC) techniques. The obtained results show that boron doped diamond on titanium substrate (Ti/BDD) anodes are promising for electrochemical treatment in the wastewater. The reducing the TOC concentration, promoted a breakdown of the carbofuran molecule, showing inorganic carbon ( $\text{CO}_2$ ,  $\text{CO}$ ,  $\text{H}_3\text{CNH}_2$ ) formation, rather than the mineralization of organic compounds. This fact may have contributed to the intermediate products formation resulting from the reaction of degradation of the pesticide.

**Keywords:** Ti/BDD electrodes; Electrochemical oxidation; Carbofuran pesticide.

### RESUMO

Eletrodos de diamante dopado com boro (BDD) foram produzidos sobre substrato de titânio (Ti) por deposição química a partir da fase vapor assistida por filamento quente (HFCVD) para degradação eletroquímica do pesticida carbofurano. As caracterizações morfológica e estrutural dos eletrodos foram analisadas por Microscopia Eletrônica de Varredura (SEM) e Espectroscopia Raman. O valor da densidade de carga aparente ( $N_A$ ) foi determinado por Mott-Schottky Plot, nos quais foram de aproximadamente  $10^{19} \text{ cm}^{-3}$ . A caracterização eletroquímica dos eletrodos foi realizada por Voltametria Cíclica e observada ampla janela de potencial. A oxidação eletroquímica do carbofurano foi realizado em diferentes densidades de corrente, com fluxo de 50 e  $300 \text{ Lh}^{-1}$  durante 2 horas com uma solução aquosa de carbofurano com concentração de  $1,8 \times 10^{-3} \text{ M}$  dissolvido em Sulfato de potássio ( $\text{K}_2\text{SO}_4$ ) 0.1 M utilizando um reator de fluxo com recirculação. A eficiência do processo de degradação do pesticida foi avaliada pelas técnicas de Espectrofotometria nas regiões Ultravioleta e Visível (UV-Vis), Carbono Orgânico Total (TOC) e Cromatografia Líquida de Alta Eficiência (HPLC). Os resultados obtidos mostraram que os anodos de diamante dopado com boro em substratos de titânio (Ti/BDD) são promissores para tratamento eletroquímico em águas residuais. A redução da concentração de TOC promoveu a quebra das moléculas do carbofurano, com formação de carbono inorgânico ( $\text{CO}_2$ ,  $\text{CO}$ ,  $\text{H}_3\text{CNH}_2$ ), ao invés da mineralização dos compostos orgânicos. Esse fato pode ter contribuído para a formação de compostos intermediários como resultado da reação de degradação do pesticida.

**Palavras - Chave:** Eletrodos de Ti/BDD; Oxidação eletroquímica; Pesticida carbofurano.

<sup>1</sup>Instituto Nacional de Pesquisas Espaciais – Coordenação dos Laboratórios Associados – Laboratório de Plasma – São José dos Campos (SP) – Brazil

<sup>2</sup>Universidade de São Paulo – Instituto de Química de São Carlos -Departamento de Química e Física Molecular – São Carlos (SP) – Brazil.

<sup>3</sup>Instituto Nacional de Pesquisas Espaciais – Coordenação dos Laboratórios Associados – Laboratório Associado de Sensores e Materiais - São José dos Campos (SP) – Brazil.

**Correspondence author:** Nazir Monteiro dos Santos – INPE/LAS – Av. dos Astronautas, 1.758, Jd. da Granja – CEP 12.227- 010 – São José dos Campos (SP) – Brazil  
E-mail: nmsmarins@yahoo.com.br

**Received:** 05/07/2015 **Approved:** 02/24/2016

## INTRODUCTION

Boron-doped diamond electrodes (BDD) are a promising material for high frequency and high-power applications like Field Emission Transistors, Schottky diodes and specially as electrode applied to electrochemical sensors, and electro-synthesis of organic and inorganic compounds<sup>(1-4)</sup>. BDD electrodes have been extensively studied for their ability to oxidize a wide range of water contaminants by a combination of direct electron transfer and reaction with hydroxyl radicals ( $\bullet\text{OH}$ ) produced from water oxidation<sup>(5-7)</sup>. To date, conductive diamond has several superior characteristics compared with other carbon materials and metals, including very low background current density and wide potential window in aqueous solution<sup>(8, 9)</sup>. The advantage of the diamond electrode is the fact that it allows the detection of redox reactions in certain potentials that would be outside the range of work potential of conventional electrodes, as platinum ( $\sim 2.0$  V), glassy carbon ( $\sim 2.5$  V), and graphite ( $\sim 2.0$  V). In this work, Ti/BDD electrodes were characterized by Scanning Electron Microscopy (SEM), Raman Scattering Spectroscopy, Mott-Schottky Plot (MSP) and Cyclic Voltammetry (CV) techniques, associating them with the electrochemical efficiencies for the degradation of the carbofuran pesticide.

Electrochemical oxidation (EO) offer viable alternatives to the more traditional methods employed in the treatment of aqueous non-biodegradable recalcitrant organic pollutants of high toxicity through oxidation by hydroxylation benzenic ring or H atom abstraction from side chain<sup>(7)</sup>. The Ti/BDD anode may be defined as non-active electrodes, where it does not participate in the anodic reactions. The hydroxyl radicals formed in the Ti/BDD anode surface are non-selective and very powerful oxidants with the ability to react with organic components until mineralization (i.e. their conversion into  $\text{CO}_2$ ,  $\text{H}_2\text{O}$  and inorganic ions) is achieved.

In EO, contaminants are destroyed after adsorption on the Ti/BDD anode surface, without involvement of any substances other than the electron, which is a clean reagent.

The carbofuran or 2,3 dihydro-2,2-dimethyl-7-benzofuran-yl-N-methyl carbamate is characterized as an insecticide and nematicide belonging to the carbamate group, widely used pesticide in most third world countries. Carbofuran is used in a rural area in southeast Brazil in rice irrigation. It is soluble in water, and through periodic applications in the same soil, it increases the degradative activity of the compound, due to the higher growth of microorganisms able to use it as a source of carbon and nitrogen<sup>(10-12)</sup>. The risks to human health by pesticides in agriculture are derived principally from its misuse. In addition to possible direct contamination in the field, the human being is still exposed to residues of pesticides present in water, air and soil. More severe poisoning by carbofuran occurs by inhalation or ingestion, and the more moderate by skin absorption<sup>(13)</sup>. The concern over the presence of pesticides in food is as old as the introduction of these chemicals to control pests that

affect agricultural production. From the environmental point of view, the carbofuran presents relatively high toxicity in mice ( $\text{LD}_{50}$  2  $\text{mgkg}^{-1}$ ) and rats ( $\text{LD}_{50}$  8-11  $\text{mgkg}^{-1}$ )<sup>(14-16)</sup>. Carbofuran is extensively used as a soil-incorporated carbamate in order to control a variety of insect pests. The action of carbofuran is due to the inhibition of acetylcholine esterase, an enzyme vital to normal nerve function<sup>(17)</sup>.

The versatility of EO process offers several possibilities with many possible pathway of the carbofuran degradation, depending on the reaction conditions and aromatic ring substitution. The carbofuran is efficiently degraded through hydrolysis of the methylcarbamate chain, causing the formation of a phenolic structure and methylamine as well as the hydrolysis of the furan ring and oxidation of the benzene ring, allowing the formation of hydroxylated structures and other metabolites<sup>(18-19)</sup>.

Because of the heavy use of carbofuran in agricultural production, this study aimed to analyze the electrochemical oxidation of commercial carbofuran (Fig. 1) through the use of Ti/BDD electrodes, and to test the electrode responses in an electrochemical flow reactor operating at different hydrodynamic conditions.

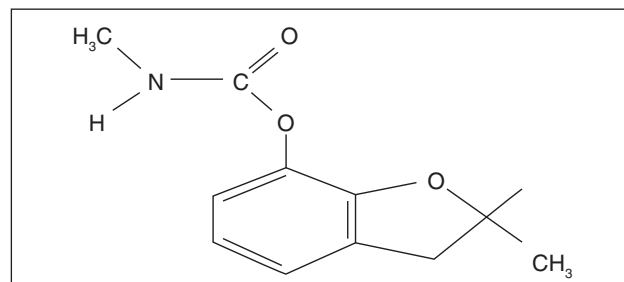


**Figure 1:** Molecular structure of carbofuran.

## EXPERIMENTAL

### Ti/BDD electrodes production and characterization

Boron-Doped Diamonds were produced on titanium substrate (Ti/BDD) by Hot Filament Chemical Vapor Deposition (HFCVD) technique on a reactor using a gas mixture of 99%v  $\text{H}_2$  and 1%v  $\text{CH}_4$  at a total flow of 200 sccm (standard centimeter cubic per second). The temperature and the pressure inside the reactor were maintained at 650 °C and 40 Torr, respectively. The distance between the filament and the substrate was 5 mm and the deposition time was 16 h. Titanium substrates were used in the dimensions of 2.5 cm  $\times$  2.5 cm. To improve the adhesion of the diamond film on the substrate and the nucleation density during growth of the films, we performed a pre-treatment on the surface of substrates, which consists of a mechanical incision by blasting with glass beads, whose main objective is increasing roughness<sup>(20)</sup>. From this, the substrates were cleaned with acetone in an ultrasonic bath in order to remove grease and any other contaminants, and soon after, prepared for growth by plating with diamond powder (0.25  $\mu\text{m}$ ) suspended in hexane for 1 h

in ultrasonic bath. For the process of production of Ti/BDD electrodes, hydrogen was passed through a bubbler containing trimethylborate  $\text{BO}_3(\text{CH}_3)_3$  dissolved in methanol ( $\text{CH}_3\text{OH}$ ), which is drawn to the entry into the reactor. The dopant solution flow was controlled by a rotameter which was kept 35 sccm, and the bubbler temperature was maintained at 30 °C. The doping process was performed during the entire period of growth of the Ti/BDD films, using a concentration of trimethylborate dissolved in methanol of the 20000 ppm of boron atoms with respect to the carbon atoms (B/C) of methanol.

The quality of Ti/BDD electrodes was investigated by Raman Spectroscopy using a Renishaw equipment model S2000, with argon ion laser at 514.5 nm using Raman shift spectra at 300 to 3000  $\text{cm}^{-1}$ . The surfaces morphology of the Ti/BDD electrodes was observed with Scanning Electron Microscopy (SEM) using the brand Microscope JEOL, model JSM-5310. The Ti/BDD electrodes were characterized by Cyclic Voltammetry to measure the working potential range (potential window) of the background current. The number of charge carriers present on the surface of diamond electrodes was determined by Mott-Schoktty Plot obtained in 0.5 M sulphuric acid ( $\text{H}_2\text{SO}_4$ ). The electrochemical measurements were performed using a Potentiostat / Galvanostat Autolab PGSTAT 302.

### Electrochemical system used in degradation process of the pesticide carbofuran

The carbofuran degradation was performed out in an electrochemical reactor comprising two parallel polypropylene plates ( $h = 25 \text{ cm}$ ,  $l = 14 \text{ cm}$ ,  $\varnothing_{\text{ext}} = 4 \text{ mm}$ ,  $\varnothing_{\text{int}} = 2 \text{ cm}$ ) equipped with four Ti/BDD anodes, four 316 L stainless steel cathodes (total geometric area 16.6  $\text{cm}^2$ ), internal spacer between cathodes and anodes was about 4 mm (Fig. 2)<sup>(21)</sup>. The reactor was connected to a recirculation system (volumetric capacity 2.5 L) thermostated at 20 °C, through which electrolytes could be supplied at recirculation flow rates of 50  $\text{Lh}^{-1}$  (laminar flow;  $\text{Re} 300$ ) or 300  $\text{Lh}^{-1}$  (turbulent flow;  $\text{Re} 1900$ ). EO reactions were carried at different applied current densities ( $J_{\text{appl}}$ ) in the range 10 to 200  $\text{mAcm}^{-2}$  for a full 2 h. As electrolyte was used 0.1 M  $\text{K}_2\text{SO}_4$  and  $1.8 \times 10^{-3}$  M carbofuran aqueous solution. The carbofuran was purchased commercially as Ralzer TS 350 (Fersol), it containing 350  $\text{gL}^{-1}$  carbofuran and 720  $\text{gL}^{-1}$  inert ingredients and coadjuvants. It is registered in the CAS (Chemical Society American) under number 1563-66-2<sup>(14)</sup>. Electrolyte was sampled at 20 min intervals in each experiment and the spectra were obtained using a Hitachi High-Technologies (Tokyo, Japan) Model U-4100 Spectrometer ( $250 \text{ nm} < \lambda < 800 \text{ nm}$ ). The concentration of pesticide in the electrolyte was monitored by High Performance Liquid Chromatography (HPLC) using a Perkin-Elmer (USA) Flexar model and a Phenomenex (Torrance, CA, USA) Luna C18 column ( $250 \text{ mm} \times 4.6 \text{ mm i.d.}$ ; 5  $\mu\text{m}$ ). Isocratic elution was with a mobile phase comprising acetonitrile and water (60:40) at a flow rate of 1.0  $\text{mLmin}^{-1}$ , and detection was at 262 nm. Quantitative analysis

of the pesticide was performed with the aid of a calibration curve constructed using carbofuran analytical standard (Sigma-Aldrich, St. Louis, MO, USA; product PS 1024 Supelco). The variation of total organic carbon (TOC) of electrolyte was measured using a Shimadzu TOC-VCPN analyzer.

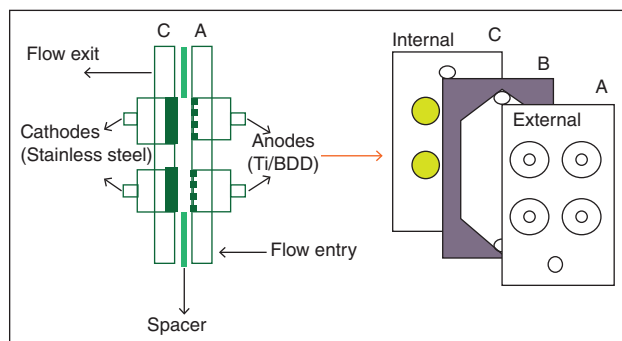


**Figure 2:** Schematic view of the electrochemical ascendant flow reactor (A) and (C), external parallel polypropylene plates fitted with four Ti/BDD anodes and four 316 L stainless steel cathodes and (B) internal spacer between cathodes and anodes.

## RESULTS AND DISCUSSION

### Morphological and structural characterization of Ti/BDD electrodes

Figure 3 shows SEM micrographs and Raman spectra of microcrystalline diamond film in the absence and in the presence of boron. Figure 3 (a, c) shows continuous and homogeneous films covering the entire substrates. The films are composed of uniformly densely packed well-faceted crystalline diamond, with many (111) faces for diamond film in the absence of boron that start to turn into a finely grained non-faceted texture on Ti/BDD electrodes. Moreover, the films strongly adhered to the substrate and showed no signs of cracks or delamination.

In general, the Raman spectroscopy has emerged as one of the most frequently used tools to characterize carbon based material<sup>(22)</sup>. Using Raman, observed changes in the behavior of C-C bonds, probing molecular structure variation due to boron incorporation and assessing crystalline quality of the Ti/BDD electrodes.

In Fig. 3b, it can be observed that the intense first order Raman peaks at 1332  $\text{cm}^{-1}$  indicating the existence of diamond crystallites. In Fig. 3d, it can be seen the band at 500  $\text{cm}^{-1}$ , the peak at 1200  $\text{cm}^{-1}$  and the broad band from 1500 to 3000  $\text{cm}^{-1}$ , that besides from the well-known characteristic diamond peak at 1332  $\text{cm}^{-1}$ . The band at 500  $\text{cm}^{-1}$  is associated with the vibration of boron pairs in the diamond lattice and the peak at 1200  $\text{cm}^{-1}$  may be attributed to disorder in the diamond structure caused by incorporation of boron<sup>(22)</sup>. The structure located in the broad band from 1500 to 3000  $\text{cm}^{-1}$  is attributed to crystalline graphite phase indicating the presence of  $\text{sp}^2$  bonded carbon, however it is not pronounced.

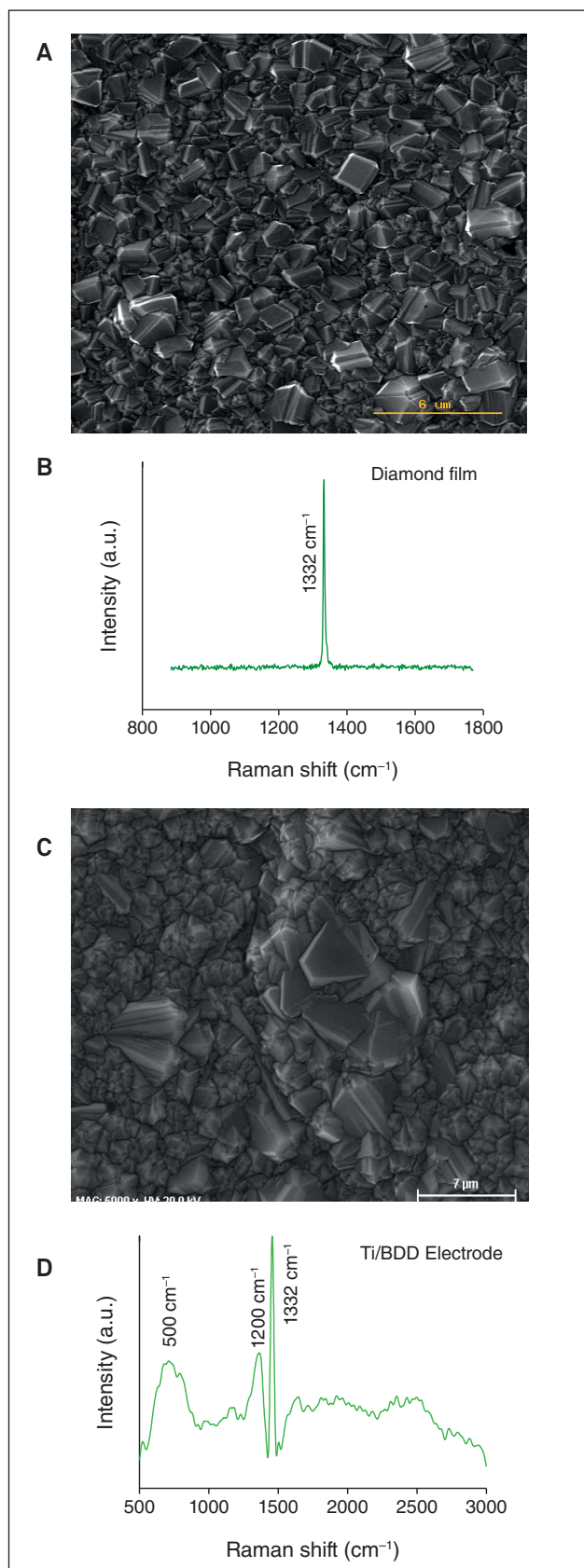


**Figure 3:** (A) SEM micrographs and (B) Raman spectra of diamond film in the absence of boron. (C) SEM micrographs and (D) Raman spectra of Ti/BDD electrodes with concentration of the 20000 ppm in B/C.

### Mott-Schottky plot and voltammetry measurements of Ti/BDD electrodes

The charge carriers concentration at the surface of the electrodes was evaluated by measuring differential capacitance in the interface Ti/BDD electrode/electrolyte through Mott-Schottky plot (MSP) curves in 0.5 M  $\text{H}_2\text{SO}_4$ . The measurements were performed at amplitude of 10 mV and frequencies of 10 kHz. This procedure has been described in detail in previous work by the group INPE Diamond<sup>(23,24)</sup>. The Ti/BDD electrode presented donor density ( $N_A$ ) values of  $6.8 \times 10^{19} \text{ cm}^{-3}$  boron atoms and the flat band potential values ( $E_{FB}$ ) was approximately at 1 V/MSE.

Figure 4 shows cyclic voltammograms of Ti/BDD electrode produced in this work. The experiments were performed in 0.5 M  $\text{H}_2\text{SO}_4$  with a scan rate of 20 mV/s, can be seen in Fig. 4a. The results reveal that the Ti/BDD electrodes have a wide range of working potential stability to water. The values obtained for the working potential window of Ti/BDD electrodes are around of 3.0 V. This value is comparable to those in the literature for diamond deposited on silicon substrates<sup>(25-27)</sup>. The advantage of the diamond electrode is the fact that it allows the detection of redox reactions in certain potentials that would be outside the range of work potential of conventional electrodes. That is, the diamond electrode allows the investigation of substances having standard potential more positive or negative without interference from the water electrolysis. The reaction of  $\text{O}_2$  generation was started at approximately 1.8 V and the reaction of  $\text{H}_2$  generating

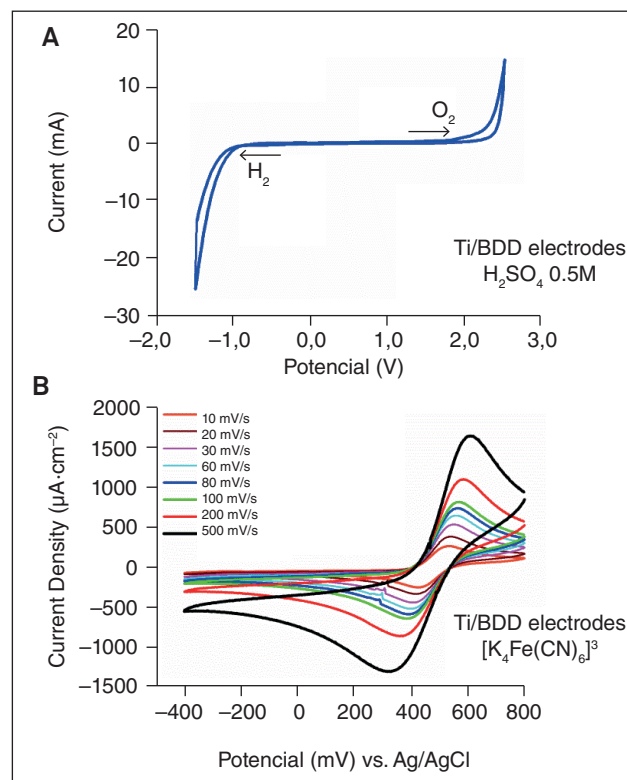


**Figure 4:** Cyclic voltammograms of the Ti/BDD electrodes in scan rate: (A) 20 mV/s in 0.5 M  $\text{H}_2\text{SO}_4$  and (B) 10 to 500 mV/s in 1.0 mM  $(\text{K}_4\text{Fe}(\text{CN})_6)^{3-}$  dissolved in 0.5 M  $\text{H}_2\text{SO}_4$  solution.

at about  $-1.0$  V. The high value of positive anodic limit of these electrodes makes them good candidates for application as anode materials for organic electro oxidation<sup>(28)</sup>. In Ti/BDD anode, organic compounds are completely oxidized via  $\bullet\text{OH}$  radical electro generated, so that these electrodes are good for use in electrochemical degradation of the pesticides and herbicides, promoting the combustion of organic pollutants with high efficiency<sup>(29)</sup>. Besides experiments were performed to study the electrochemical kinetics of the electrodes, by varying the scan rate from 10 to 500 mV/s in potassium ferricyanide solution ( $(\text{K}_4\text{Fe}(\text{CN})_6)^{3-}$ ), as can be seen in Fig. 4b. The aim was to determine the response of Ti/BDD electrodes according to the criteria of reversibility of redox reactions. The direct observation in Fig. 4b, shows that increasing the scan rate potential the cathodic and anodic peaks, current density also increases. The cathodic and anodic peaks arise due to charge transfer reactions (oxidation and reduction) of one electron,  $(\text{K}_4\text{Fe}(\text{CN})_6)^{3-/4-}$ , during the application cycle potential. According to reversibility results, the electrodes Ti/BDD have the characteristics of almost reversibility. This confirmation is made by observing criteria as the separation between anodic and cathodic peaks<sup>(30)</sup>.

Figure 5 shows the cyclic voltammograms of the Ti/BDD electrodes in  $0.1$  M  $\text{K}_2\text{SO}_4$  (supporting electrolyte in the pesticide degradation) and  $1.8 \times 10^{-3}$  M carbofuran solution. In the Fig. 5a, it is observed that the  $\text{O}_2$  generation reaction began at approximately  $1.5$  V when using  $0.1$  M  $\text{K}_2\text{SO}_4$  solution, and in the presence of carbofuran the  $\text{O}_2$  generation reaction started at  $2.2$  V, as can be seen

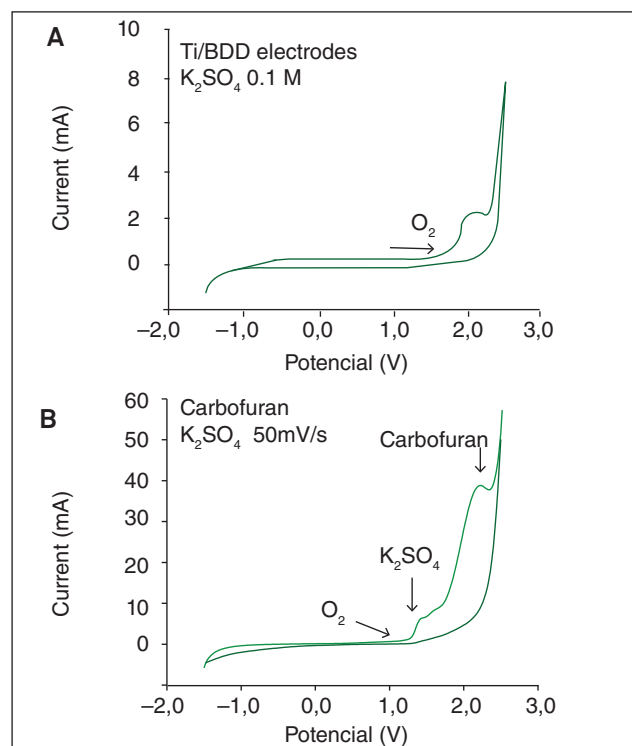


**Figure 5:** Cyclic voltammograms of Ti/BDD electrodes at scan rates of  $50$  mV/s in  $0.1$  M  $\text{K}_2\text{SO}_4$  (A) and  $1.8 \times 10^{-3}$  M carbofuran dissolved in  $0.1$  M  $\text{K}_2\text{SO}_4$  solution (B).

in Fig. 5b. The appearance of these oxidation peaks indicates that the carbofuran is electroactive at the surface of Ti/BDD electrodes. This effect facilitates competition with the oxygen evolution reaction, improving the efficiency of electrochemical oxidation.

### UV/Vis analysis of the electrochemical oxidation process of the pesticide

The electrochemical oxidation (EO) of carbofuran was monitored by using UV/Vis spectroscopy in order to obtain the absorbance as a function of wavelength ( $\lambda$ ) of the samples collected during the procedure. It was performed with laminar recirculation flow ( $50$  Lh<sup>-1</sup>) condition and at different current density of  $10$ ,  $50$ ,  $100$  and  $200$  mAcm<sup>-2</sup>. Figure 6 presents the UV/Vis spectra of samples collected before of the EO (T0) and  $10$  min (T10) to  $120$  min (T120) after EO process. Notice that the samples absorbance occurred at the maximum peak wavelength of  $276$  nm and that variation could be detected after the first few minutes of the EO process.

It is observed in Fig. 6 (C) and (D), the emergence of a new spectral band ( $290 < \lambda < 400$  nm) when was used higher current densities ( $100$  and  $200$  mAcm<sup>-2</sup>). Band intensity increases due to the intermediate compounds formation, such as: 3-hydroxy-carbofuran ( $\text{LD}_{50}$   $18$  mgkg<sup>-1</sup>), 3- keto-carbofuran ( $\text{LD}_{50}$   $69$  mgkg<sup>-1</sup>), 7-phenol ( $\text{LD}_{50}$   $2200$  mgkg<sup>-1</sup>), 3-hidroxy-7-phenol ( $\text{LD}_{50}$   $1350$  mgkg<sup>-1</sup>) and 3-keto-7-phenol ( $\text{LD}_{50}$   $295$  mgkg<sup>-1</sup>), promoted by the attack of hydroxyl radicals formed at the BDD anode surface<sup>(14)</sup>. The 3-hidroxy-carbofuran intermediate has a half-life of the third of carbofuran half-life, but has almost the same toxicity while the other intermediates present low toxicity in the environment<sup>(31)</sup>. Figure 7 shows the absorbance at wavelength ( $276$  nm) peak as a function of current density for EO process, from the laminar ( $50$  Lh<sup>-1</sup>) and turbulent ( $300$  Lh<sup>-1</sup>) regimes. In Fig. 7a, it can be seen observed an increase in absorbance when using higher current density ( $200$  mAcm<sup>-2</sup>) in laminar regime. However, it was observed that there was no significant variation in the absorbance of the pesticide when was used a current density at  $100$  mAcm<sup>-2</sup>. At this current, there was a balance between the concentration of the starting material and the formation of intermediate compounds. In Fig. 7b, it can be shown that the absorbance increases in the first minutes ( $J_{\text{appl}} = 10$  mAcm<sup>-2</sup>) and the decreases along the EO process ( $50$  mAcm<sup>-2</sup>  $\leq J_{\text{appl}} \leq 200$  mAcm<sup>-2</sup>). The increase in concentration of carbofuran still needs to be investigated; however we can infer that it may be due to the diffusion coefficient, especially when the EO process is controlled by diffusion and no mineralization mechanism<sup>(32)</sup>. Based on these results, it may be said that the increased current density accelerates the EO process and turbulent regime is more efficient due to the benzene ring hydroxylation or abstraction of H atoms in the chain going to the oxidative cleavage of bonds with the formation of short chain, causing the decrease in toxicity of the pesticide<sup>(14)</sup>.

The results presented in Fig. 8 shows the chromatograms in laminar and turbulent regimes at  $200$  mAcm<sup>-2</sup>. Fig. 8a it is observed

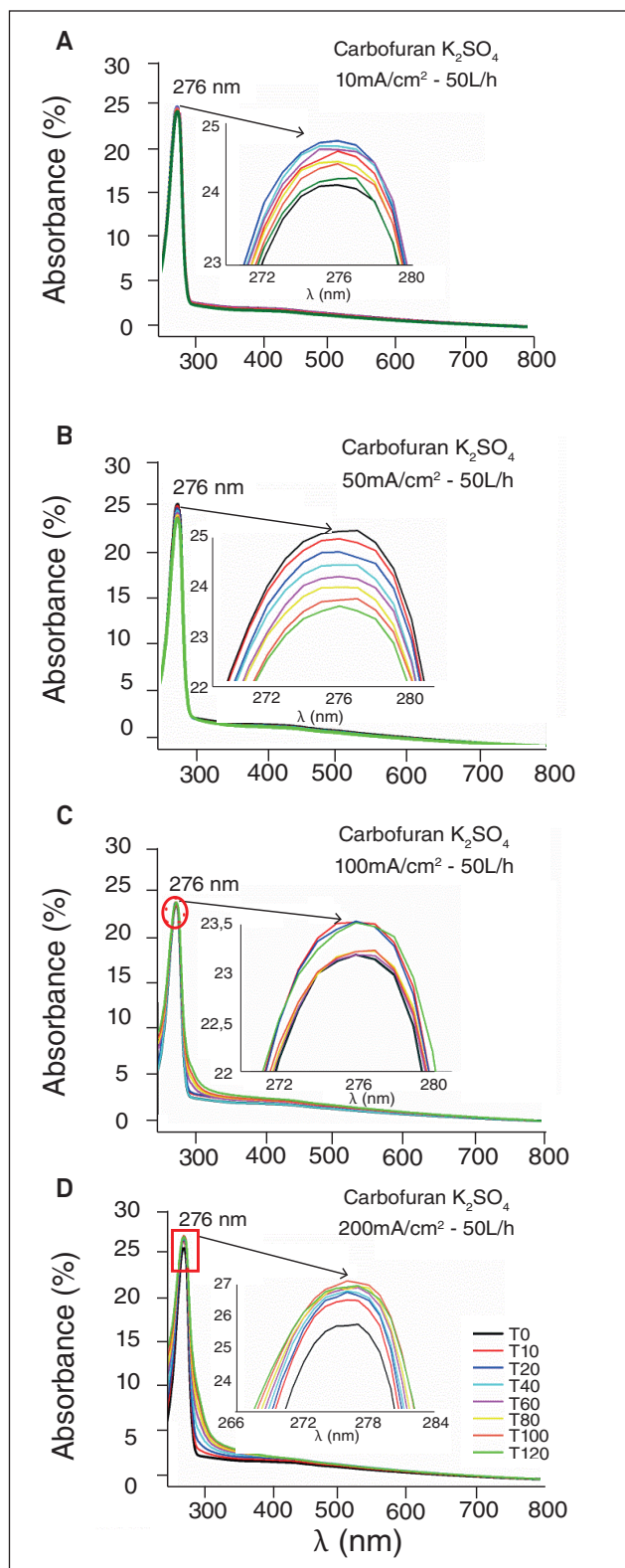


**Figure 6:** UV/Vis spectra obtained of electrolyte samples at different current densities ( $j_{appl}$ ): (A) 10 mAcm<sup>-2</sup>, (B) 50 mAcm<sup>-2</sup>, (C) 100 mAcm<sup>-2</sup> and (D) 200 mAcm<sup>-2</sup>.

two peaks of retention times (RT) at 2.12 min and 4.12 min, with variation in the absorbance as a function of degradation time. The peak related to the RT at 4.12 min corresponds to the commercial

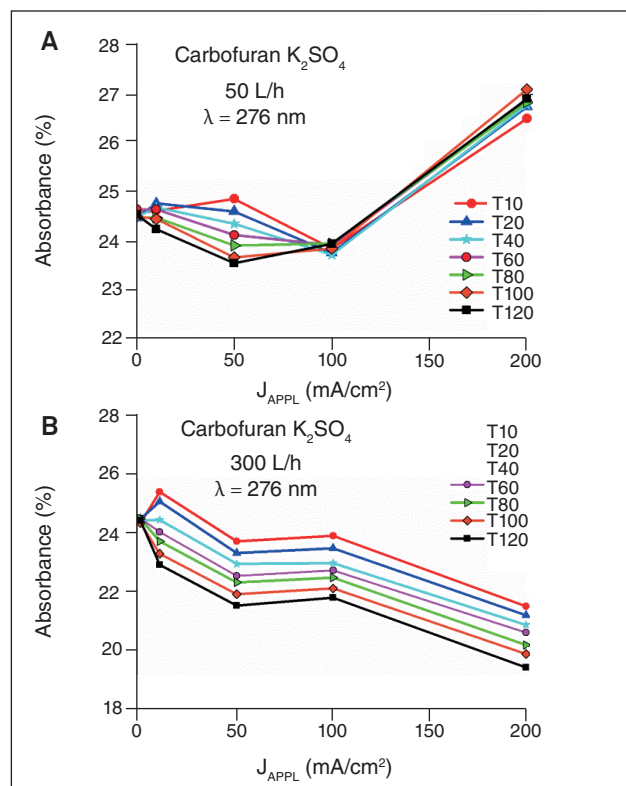


**Figure 7:** Effect of recirculation flow on the variation of absorbance as function a current density from 276 nm, (A) laminar and (B) turbulent flows.

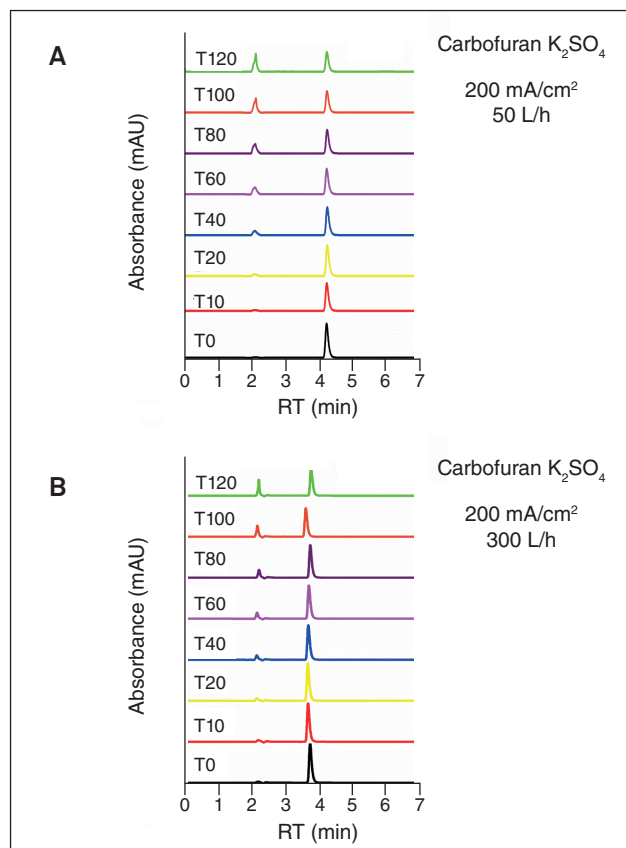


**Figure 8:** Chromatograms of carbofuran pesticide as function EO time, (A) laminar and (B) turbulent regimes.

carbofuran, had greater interaction with the stationary phase. The RT 2.12 min peak refers to inorganic compound formed along EO process. In Fig. 8b, it can be seen that in turbulent flow occurs a shift in the peak at RT = 4.12 min and decrease in absorbance. At the same time, there is an increase in absorbance peak RT = 2.12 min which has lower polarity than the initial molecule of the pesticide. This change is due to oxidation of carbofuran with formation of intermediate products with less interaction with the stationary phase. In the turbulent regime, occurs a greater removal of oxidized species of the surface of the electrode and also a better replacement of new species at the electrode/electrolyte interface; improving the efficiency of the EO process.

Figure 9 shows the results obtained from the analysis of TOC along EO process of the carbofuran. In Fig. 9a, it is observed that TOC removal concentration had little variation in the applied current densities between 10 and 50 mA/cm<sup>2</sup> and its concentration increased for current density to higher than 100 mA/cm<sup>2</sup>. In the laminar regime, the formation of inorganic carbon increased around 8% using higher current density, so there was no total degradation of the pesticide. However, intermediate products can be formed with less toxicity than carbofuran. It can be seen in Fig. 9b the efficiency of the mineralization of organic compounds in the carbofuran solution in turbulent regime (300 Lh<sup>-1</sup>). This is due to higher amount of OH• formed on the surface of the Ti/BDD anode from the oxidation of water (Equation 1).

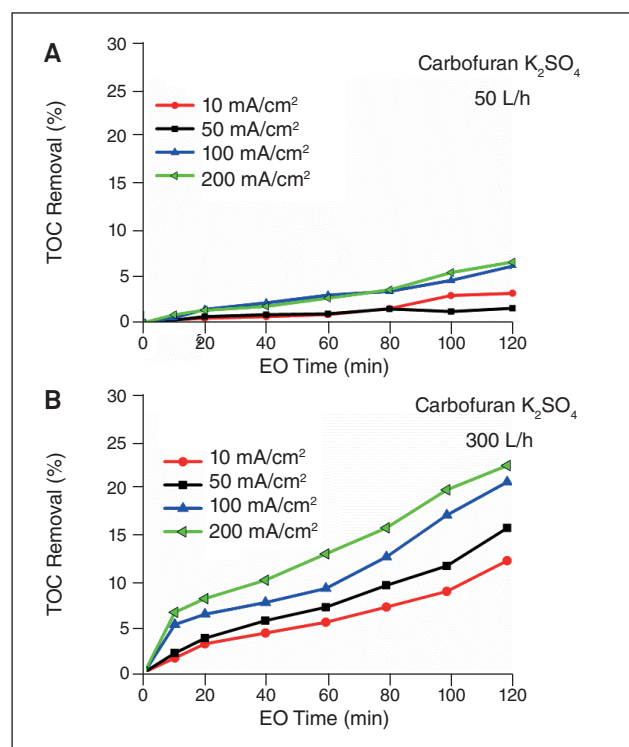
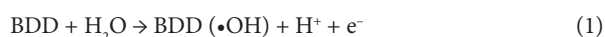


**Figure 9:** TOC removal as a function of current density along EO time, (A) laminar and (B) turbulent regimes.

However, the degradation process provided a TOC removal of ~ 25%, most current density applied along EO process indicating a partial degradation of the carbofuran with formation of short persistence intermediates in the environment and lower degree of toxicity.

## CONCLUSIONS

It can be concluded that the EO processes using Ti/BDD anode could be efficiently applied to remove pesticide and the increasing current density accelerates the degradation and mineralization processes, but with a loss in mineralization current efficiency due to the side reaction and energy loss on the persistent byproducts produced. The EO process is very promising for use in an up flow reactor because its mechanism of action occurs by adsorption of hydroxyl radicals on the surface of Ti/BDD anodes. The aromatic intermediates were oxidized at the early stage by addition of <sup>-</sup>OH on the benzenic ring (hydroxylation) or by H atom abstraction from side chain. Then, the oxidative cleavage of polyhydroxylated aromatic derivatives conducts to the formation of short chain, causing the decrease of solution toxicity. The results evaluation showed that the EO conducted at a flow rate of 300 Lh<sup>-1</sup> (turbulent hydrodynamic regime, Re = 4500) was the most effective for the degradation of carbofuran. In the turbulent regime there is greater replenishment of new species at the electrode/electrolyte interface, improving the EO process of carbofuran molecules on the surface of Ti/BDD anodes. The applied current density is one of the parameters that affect significantly the EO process. For higher current density (200 mA/cm<sup>2</sup>) was increased at the rate of oxidation and cleavage of carbofuran molecule. The electrochemical oxidation time (120 min) was not prevalent for the mineralization of the pesticide; however there was formation of others chemical compounds with less toxicity than the starting products.

## ACKNOWLEDGEMENT

The authors gratefully acknowledge the following Brazilian funding authorities for financial support: FAPESP (Proc. 2012/07326-6), CAPES and CNPq (Proc. 151.291/2014-4).

## REFERENCES

1. CHAPLIN, B.P.; HUBLER, D.K.; FARRELL, J., Understanding Anodic Wear at Boron Doped Diamond Film Electrodes, *Electrochim. Acta*, 89 (2013) 122.
2. KRAFT, A.; Doped Diamond: A Compact Review on a New, Versatile Electrode Material, *Int. J. Electrochem. Sci.*, 2 (2007) 355.
3. GANDINI, D.; MABÉ, E.; MICGAUD, P. A.; HAENNI, W.; PERRET, A.; COMNINELLIS, CH., Oxidation of Carboxylic Acids at Boron-Doped Diamond Electrodes for Wastewater Treatment, *J. Appl. Electrochem.*, 30 (2000) 1345.

4. SUFFREDINI, H.B.; MACHADO, S. A. S.; AVACA, L. A.; BRAZ, J.; The Water Decomposition Reactions on Boron-Doped Diamond Electrodes, *Chem. Soc.*, 15 (2004) 16.
5. CHAPLIN, B. P.; SCHARADER, G.; FARRELL, J., Electrochemical Destruction of N-Nitrosodimethylamine in Reverse Osmosis Concentrates Using Boron-Doped Diamond Film Electrodes, *Env. Sci. Technol.*, 44 (2010) 4264.
6. KAPALKA, A.; FOTI, G.; COMNINELLIS, C., Investigation of the Anodic Oxidation of Acetic Acid on Boron-Doped Diamond Electrodes, *J. Electrochem. Soc.*, 155 (2008) E27.
7. CANIZARES, P.; SAEZ, C.; LOBATO, J.; RODRIGO, M. A, Electrochemical Treatment of 2,4-Dinitrophenol Aqueous Wastes Using Boron-Doped Diamond Anodes, *Electrochim. Acta*, 49 (2004) 4641.
8. ZHANG, Y.; WEI, K.; W.; HAN, SUN, X.; LI, J.; SHEN, J.; WANG, L., Improved Electrochemical Oxidation of Tricyclazole from Aqueous Solution by Enhancing Mass Transfer in a Tubular Porous Electrode Electrocatalytic Reactor, *Electrochim. Acta*, 189 (2016) 8.
9. KONDO, T.; HONDA, K.; TRYK, D.A.; FUJISHIMA, A., AC Impedance Studies of Anodically Treated Polycrystalline and Homoepitaxial Boron-Doped Diamond Electrodes, *Electrochim. Acta*, 48 (2003) 2739.
10. FELSOT, A.; MADDOX, J. V.; BRUCE, W., Enhanced Microbial Degradation of Carbofuran in Soils with Histories of Furan Use, *Bull. Environ. Contam. Toxicol.*, 26 (1981) 781.
11. DHANASEKARA, S.A.K.M.; ATTANAYAKE, A.N.B.; HERATH, A. C.; NANAYAKKARA, N.; SENARATNE, A.; INDRARATHNE, S.P.; WEERASOORIYA, R., Partial Degradation of Carbofuran by Natural Pyrite, *Environ. Nanotechn., Monitoring & Management*, 4 (2015) 57.
12. PARKIN, T. B.; SHELTON, D. R., Modeling Environmental Effects on Enhanced Carbofuran Degradation, *Pestic. Sci.*, 40 (1994) 163.
13. FELSOT, A. S., Enhanced Biodegradation of Insecticides in Soil: Implications for Agroecosystems, *Ann. Rev. Entomol.*, 34 (1989) 453.
14. TOMLIN, C. D. S., *The Pesticide Manual*, Ed. Farnham: British Crop Protection Council, 2001.
15. HARTLEY, D.; KIDD H., (eds.), *The Agrochemicals Handbook*, 2nd ed. Lechworth, Herts, England: The Royal Society of Chemistry, (1987).
16. NIOSH Pocket Guide to Chemical Hazards, DHHS (NIOSH) Publication n°. 97-140, Washington, D. C. U. S. Government Printing Office, (1997).
17. ČOLOVIĆ, M. B ; KRSTIĆ, D. Z.; LAZAREVIĆ-PAŠTI, T. D.; BONDŽIĆ, A. M.; VASIĆ, V. M., Acetylcholinesterase Inhibitors: Pharmacology and Toxicology, *Curr. Neuropharmacol.* 11 (2013) 315.
18. MAHALAKSHMI, M.; ARABINDOO, B.; PALANICHAMY, M.; MURUGESAN, V., Photocatalytic Degradation of Carbofuran Using Semiconductor Oxides, *J. Hazardous Mat.*, 143 (2007) 240.
19. LU, L.A.; MA, Y.S.; KUMAR, M.; LIN, J. G., Photochemical Degradation of Carbofuran and Elucidation of Removal Mechanism, *Chem. Eng. J.*, 166 (2011) 150.
20. AZEVEDO, A. F.; CORAT, E. J.; LEITE, N. F.; TRAVA-AIROLDI, V. J., Chemical Vapor Deposition Diamond Thin Films Growth on Ti6AL4V Using the Surfatron System, *Diamond Relat. Mater.* 11 (2002) 550.
21. CORDEIRO, G. S.; ROCHA, R. S.; VALIM, R. B.; MIGLIORINI, F. L.; BALDAN, M. R.; LANZA, M. R. V.; FERREIRA, N. G., Degradation of Profenofos in an Electrochemical Flow Reactor Using Boron-Doped Diamond Anodes, *Diamond Relat. Mater.*, 32 (2013) 54.
22. KAVAN, L.; ZIVCOVA, Z. V.; PETRAK, V.; FRANK, O.; JANDA, P.; TARABKOVA, H.; NESLADEK, M.; MORTET, V.T., Boron-Doped Diamond Electrodes: Electrochemical, Atomic Force Microscopy and Raman Study Towards Corrosion-Modifications at Nanoscale *Electrochim. Acta*, 179 (2015) 626.
23. FERREIRA, N. G.; SILVA, L. L. G.; CORAT, E. J.; TRAVA-AIROLDI, V. J.; IHA, K., Electrochemical Characterization on Semiconductors p-Type CVD Diamond Electrodes, *Bra. J. Phys.*, 29 (1999) 760.
24. MATSUSHIMA, J. T.; SANTOS, L. C. D.; COUTO, A. B.; BALDAN, M. R.; FERREIRA, N. G., Influência do Eletrólito na Eletrodeposição de Nanopartículas de Cu sobre Eletrodo de Diamante Dopado com Boro, *Química Nova*, 35 (2012) 11.
25. RYL, J.; BURCZYK, L.; BOGDANOWICZ, R.; SOBASZEK, M.; DAROWICKI, K., Study on Surface Termination of Boron-Doped Diamond Electrodes Under Anodic Polarization in H<sub>2</sub>SO<sub>4</sub> by Means of Dynamic Impedance Technique, *Carbon*, 96 (2016) 1093.
26. WANG, S.; SWOPE, V. M.; BUTLER, J. E.; FEYGELSON, T.; SWAIN, G. M., The Structural and Electrochemical Properties of Boron-Doped Nanocrystalline Diamond Thin Film Electrodes Grown from Ar-Rich and H<sub>2</sub>-Rich Source Gases, *Diamond Relat. Mater.*, 18 (2009) 669.
27. GRANGER, M. C.; XU, J. S.; STROJEK, J. W.; SWAIN, J. M., Polycrystalline Diamond Electrodes: Basic Properties and Applications as Amperometric Detectors in Flow Injection Analysis and Liquid Chromatography, *Anal. Chim. Acta*, 397 (1999) 145.
28. DINIZ, A. V.; FERREIRA, N. G.; CORAT, E. J.; TRAVA-AIROLDI, V. J., Efficiency Study of Perforated Diamond Electrodes for Organic Compounds Oxidation Process, *Diamond Relat. Mater.*, 12 (2003) 577.
29. FÓTI, G.; GANDINI, D.; COMNINELLIS, C.; PERRET, A.; HAENNI, W., Oxidation of Organics by Intermediates of Water Discharge on IrO<sub>2</sub> and Synthetic Diamond Anodes, *Electrochem. Sol.-State Let.*, 2 (1999) 228.
30. GREEF, R.; PEAT, R.; PETER, L.M.; PLETCHER, D.; ROBINSON, J., *Instrumental Methods in Electrochemistry*, New York: John Wiley & Sons, 443 (1985).
31. FMC, Carbofuran Data Summary, Philadelphia: FMC Corporation, (1977) 97.
32. BALEK, V.; RAO, TATA, N. RAO; TRYK, D.A.; FUJISHIMA, A.; Diffusion Structural Diagnostics of Polycrystalline Boron-Doped Diamond Films, *Thermochim. Acta*, 524 (2011) 104.